A Late Holocene case study from south-west France: Combining geomorphology and geophysics to understand archaeological site morphology

Marie Larcanché, Cécile Verdet, Colette Sirieix, Ronan Steinmann, Sylvain Colin, Vivien Mathé, Christian Chevillot, Sylvain Matéo, Nicolas Houillon, Juliette Hantrais, et al.

Received: 2 March 2023 | Revised: 24 July 2023 | Accepted: 15 September 2023

DOI: 10.1002/arp.1913

RESEARCH ARTICLE

WILEY

A Late Holocene case study from south-west France: Combining geomorphology and geophysics to understand archaeological site morphology

Marie Larcanché[1] | Cécile Verdet[1] | Colette Sirieix[1] | Ronan Steinmann[2] | Sylvain Colin[3] | Vivien Mathé[4] | Christian Chevillot[5] | Sylvain Matéo[1] | Nicolas Houillon[1] | Juliette Hantrais[6] | Eneko Hiriart[6]

[1]CNRS, UMR 5295, University of Bordeaux, Talence, France

[2]Hadès – Archaeological investigations, France (geoarchaeologist) and ARTEHIS UMR 6298 CNRS, University of Burgundy, Dijon, France

[3]Hadès – Archaeological Investigations, Paris, France

[4]UMR 7266 LIENSs, University of La Rochelle, Talence, France

[5]UMR 6566 CReAAH, CNRS, University of Rennes 1, Talence, France

[6]CNRS, UMR 6034, University of Bordeaux-Montaigne, Talence, France

Correspondence
Marie Larcanché, CNRS, UMR 5295, University of Bordeaux, I2M Bordeaux, 33400 Talence, France.
Email: marie.larcanche@u-bordeaux.fr

Funding information
Université Bordeaux Montaigne; New Aquitaine region (RAPSODIE project); DRAC (Ministry of Culture) General Council of the Dordogne; University of Bordeaux Montaigne; GPR Human Past

Abstract

This article combining geophysics and archaeology aims to provide a more comprehensive characterization of the La Ruchelle valley located in the south of the Celtic site of La Peyrouse (Saint-Félix-de-Villadeix, Dordogne, France) (occupied between the 3rd century BC and the 2nd century AD) through geological prospection (core sampling, geotechnical prospection and mechanical prospection) and near-surface geophysics (electrical resistivity tomography). On this site, other studies have been carried out since the discovery of the site, such as magnetic prospecting and a hydrogeological study. Geophysical data coupled with geological prospection were used to understand the geology of the valley: (1) The bottom of the valley is filled with colluvium with a thickness of 6 m maximum; (2) part of the colluvium filling characterize by a very low resistivity is indeed archaeological remains; (3) three very distinct geological horizons have been detected—two of these horizons are characteristic of Campanian limestone (C6d and C6e), and the last consists of colluvium with a filling between 2 and 6 m in the centre of the valley, which is particularly thick. This last very thick formation is in fact filled with archaeological and prehistoric remains.

KEYWORDS
archaeological remains, archaeological stratigraphy, bedrock detection, colluvial filling, electrical resistivity tomography (2D and 3D)

1 | INTRODUCTION

In recent years, archaeological prospecting has seen major advances using a variety of remote sensing and computer technologies. Geophysical instrumentation continues to improve its sensitivity and acquisition speed, and new multi-sensor arrays, for example, pulled by carts on land, now allow large areas to be covered quickly (Deiana et al., 2018). The geoelectric resistivity technique is a well-known geophysical method, generally used in geology particularly in prehistoric site, for the non-invasive investigation of the subsoil (Xu et al., 2015). This method allows obtaining detailed images on the lateral and vertical distribution of electrical resistivity in the studied part of the subsoil, using advanced, efficient and reliable 2D and 3D inversion algorithms (Abu-Zeid, 2002; Jongmans & Garambois, 2007). Other

authors have drawn attention to the relationship between geophysics and archaeology (Apostolopoulos & Kapetanios, 2021; Becker, 1995; Dalan & Banerjee, 1996; Eppelbaum et al., 2001; Leucci et al., 2016; Querrien et al., 2009; Trinks et al., 2018; Tsourlos & Tsokas, 2011), demonstrating the potential of magnetism, soil GPR for archaeological studies but also that electrical resistivity tomography (ERT) is a valuable method for the investigation of underground structures and archaeological features. ERT and ground penetrating radar are also capable of detecting subsurface cavities (Hojat et al., 2020; Kofman et al., 2006; Park et al., 2014; Rousset et al., 1998).

The La Peyrouse site is located in the south-west of France in the Dordogne department (Figure 1). This site is mainly divided into two geological sectors. The first corresponds to the Campanian limestone plateau, which today encompasses almost the entire study site. The second sector is located south of the limestone plateau and feature a valley called 'La Ruchelle' and a filled cave (yellow triangle on the Figure 1). In this article, only the second sector is studied (represented by a blue circle in Figure 1). The La Ruchelle valley was initially studied as part of the construction of a water reserve in 2017 by geotechnical surveys, revealing archaeological remains at a depth of 3 m covered by layers of colluvium several meters thick. Indeed, this site in La Ruchelle valley was previously known for archaeological remains discovered in 2014 both on the plateau and in the cave located higher up around 150 m above sea level. The remains are mainly dated not only to the Second Iron Age (Hiriart et al., 2022), corresponding to the Celtic period (approximately 3rd century BC) but also to the Roman period (about 2000 years BC). The geomorphological study of the site will provide an important aid to archaeology to know where to prospect and whether there is the probability of finding archaeological remains. Geophysics makes it possible to cover larger expanses of land than simple boreholes or punctual excavations of a site. The geophysical prospection is completed with geological prospection. Since 2014 on the site of La Peyrouse, numerous geological surveys have been carried out, such as coring and excavations. This paper aims to illustrate the utility of this type of prospecting.

In this article, two geophysical methods are used: (i) ERT that gives an image of the electrical property of the subsoil. The 3D ERT aims at assessing the extent and rough shape of the filled cave as

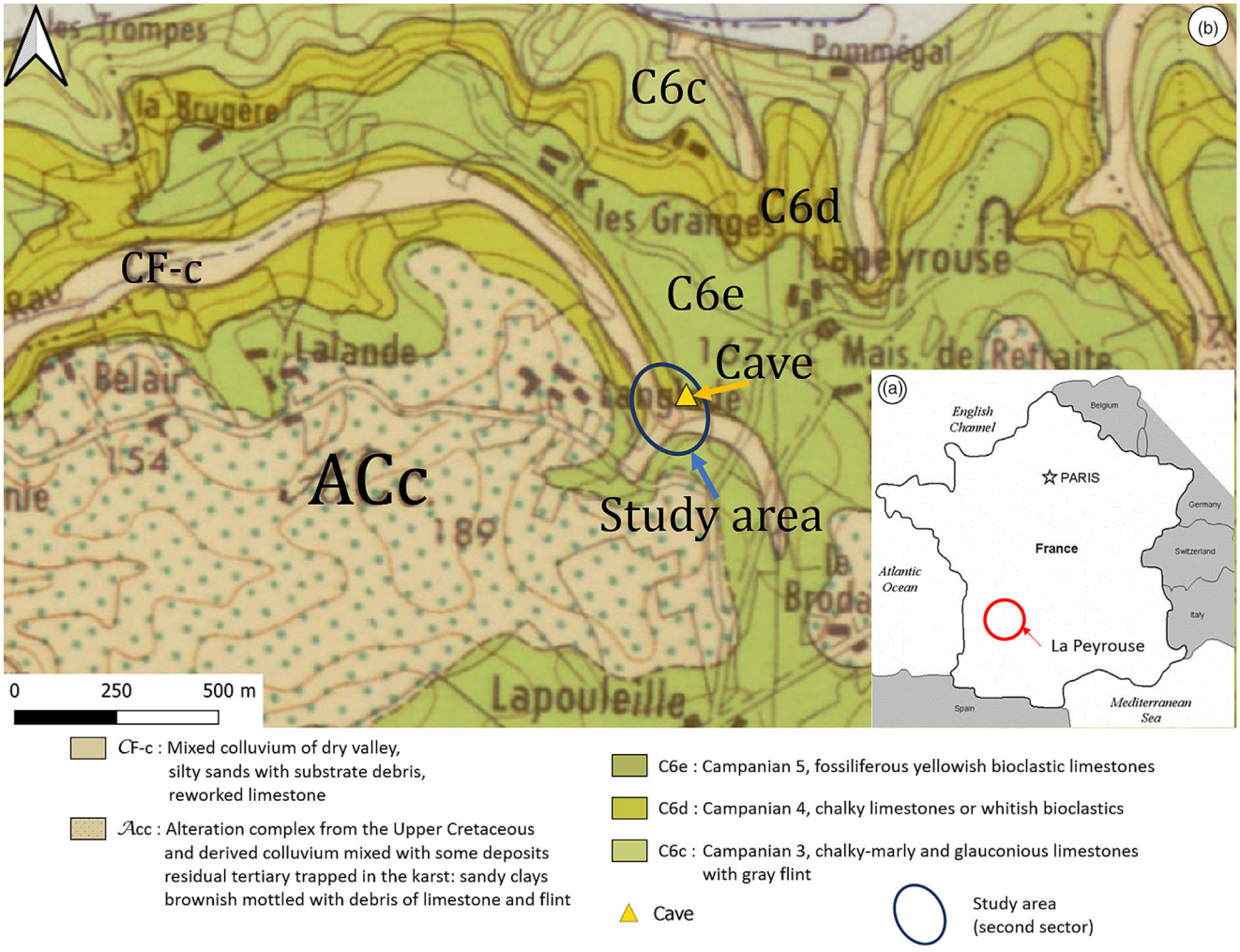

FIGURE 1 (a) Study area location and (b) geological map of La Peyrouse site (BERGERAC no. 182 at 1/50 000).

Verdet et al. (2020) and Xu et al. (2016) have shown that it is possible to create a 3D geostatistical model from 2D ERT data. (ii) A magnetic prospection was carried out in 2019 on the limestone plateau. The methods used for geological prospection on the La Peyrouse site are coring and mechanical prospection. The objectives of this study are to (i) determine the extension of the cave as it could contain archaeological features and (ii) assess the depth and nature of the La Ruchelle valley filling. Both objectives will use the combination of geophysics and geomorphology.

2 | REGIONAL SETTING

2.1 | Geology

La Peyrouse sits on a limestone plateau (Figure 1b) surrounded by the Caudeau valley to the north and the La Ruchelle valley to the south. The La Ruchelle valley is studied with two specific objectives in mind, namely, to understand and identify the composition of colluvial and cave filling. The valley cuts two types of limestone: The first is Campanian 5 (C6e), defined as fossiliferous yellowish bioclastic limestone, and the second is Campanian 4 (C6d), a chalky or whitish bioclastic limestone. The roof of the C6d limestone is around 160 m above sea level north of the site and between 150 and 160 m above sea level at the level of the site according to the geological map (Figure 1b). The valley is filled with mixed colluvion (CF-c), identified as silty sands with substrate debris and reworked limestone. A karstic cavity was listed on the site and explored in part by clearing, and archaeological material was discovered. The clay-sandy material was partly removed, which led to the discovery of archaeological material. Following this discovery, cave desobstruction was halted, leaving unknown the extent of the cave beyond 8 m. This cave seems to be located at the limit between the C6d and C6e limestones.

2.2 | Archaeology

The site of La Peyrouse, occupied between the 3rd BC and the 2nd century AD, is one of the oldest cities known to date in temperate Europe. This settlement, which extends over several hectares, has a strong commercial and artisanal vocation. The presence of an important long-distance road probably contributed to its economic influence. Archaeological excavations revealed a Celtic sanctuary located on the summit of the site. (1) The presence of a cave is attested in the very heart of the agglomeration. Due to its location, we can envisage a strong archaeological potential for this cavity, which is largely sealed, and we will try to determine its depth, volume and size. (2) In the middle of the valley, Iron Age levels have been found at a depth of 3 m. These observations raise many questions as to why so much sediment was deposited in almost 2000 years. All these observations will allow us to evaluate the evolution of the environment over time, by measuring the impact of human activities and climate. Thus, this site has many archaeological remains on the limestone plateau, in the cave and in the valley of La Ruchelle.

3 | MATERIALS AND METHODS

In order to present a comprehensive characterization of the La Peyrouse valley, numerous methods are used such as ERT and geological prospection. The use of these two different methods has many advantages, such as combining destructive field data with data measured via electrical methods (non-destructive data). The comparison of these two methods enables a more precise interpretation of the study area, reducing ambiguities of interpretation and providing a better understanding of geomorphology of the La Ruchelle valley.

3.1 | Geological prospection

In this study area, three geological prospection methods are used to characterize the subsurface. These methods are core sampling, surveys with mechanical shovel and excavations with mechanical shovel. The core sampling is frequently applied in geomorphological research for the following reasons: to analyse the stratigraphic sequences of different sediment and rock properties (e.g., soil depth, bulk density, water/ice content, pollen etc.), to measure sediment thickness and total depth to bedrock and to extract and analyse organic material or specific sediment/ice layers (e.g., peat, fossil organic layers, macro fossils, feldspar or quartz grains) for dating purposes (14C, optically stimulated luminescence) (Schrott et al., 2013). This method makes it possible to take samples of geological layers in tubes, enabling the non-destruction of geological strata. The surveys and excavations with mechanical shovel use a mechanical shovel to extract the soil destructively. The location of the various geological prospections is given on Figure 2. Cores C1–C7 were dug along ERT P1; C10–C12 were dug in the sediments filling if the cave. C3 and C20 are in the heart of the valley, and cores C40 and C8 are at the edge of the valley. These cores were taken after profile P1.

3.2 | Electrical resistivity tomography

ERT is one of the most popular techniques to characterize the shallow subsurface and is applied in hydrogeological, engineering or agricultural research (Binley et al., 2016; Carrière & Chalikakis, 2022; Gunther & Rucker, 2012). ERT is an active and non-destructive method used to obtain high-resolution images of subsurface patterns of electrical resistivity (Perrone et al., 2004). ERT consists of injecting a known electric current with two current electrodes. The potential difference generated by the injected current is measured with two other electrodes. The potential difference measured depends on the resistivity of the material, the intensity of the injected current and

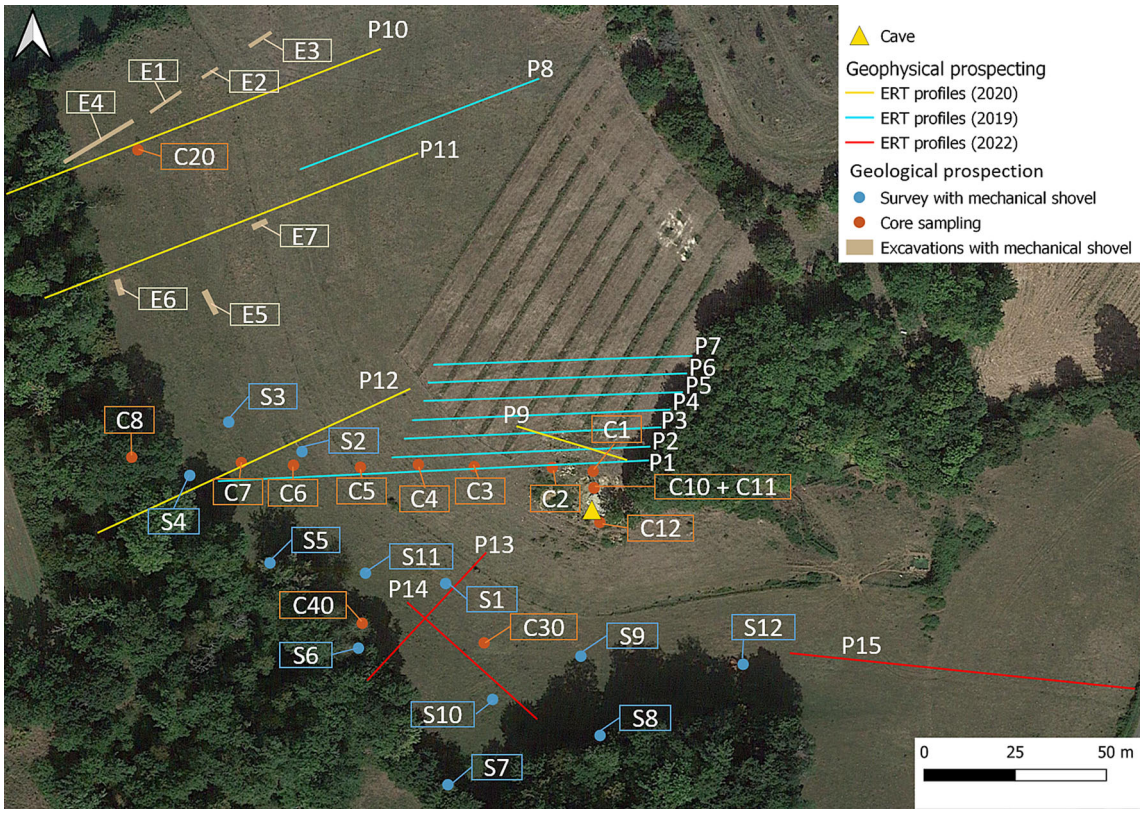

FIGURE 2 Location of 15 ERT profiles and of the geological prospection. E: excavations with mechanical shovel, C: core sampling, S: survey with mechanical shovel.

the geometry of the quadrupole used. The method is based on a multielectrode and multicable system; each of the electrodes acts alternately as a current and potential electrode, and the whole profile is measured without the intervention of surveyors (Pánek et al., 2010). In order to make the ERT measurements, sequences of measurements are programmed (Dahlin, 2000).

In the study, the inversion software used RES2DINV® (v. 4.05.38) (as per Loke & Barker, 1996), whose chosen inversion parameters (refined mesh at half the inter-electrode spacing, inversion with the L1 norm, fine mesh) allowed a particularly detailed interpretation of the profile. The L1 norm is used here because it is adapted to a heterogeneous medium where the variations of resistivities can change very quickly and the modifications of the mesh make it possible to reduce the influence of the blocks due to the inversion process. In the La Peyrouse valley, 15 ERT profiles were produced from 2019 to 2022 (Figure 2). Among these profiles, eight were produced in 2019, four in 2020 and three in 2022. The characteristics of each profile are given in Table 1. The measuring used for the ERT profiles in both 2019 and 2022 is the SYSCAL SWITCH PRO by Iris Instruments, with a TERRAMETER LS by Abem used for the measurements in 2020.

Each profile was located according to the previous geological hypothesis: P1–P7 are placed where we assume the cave is with a space of 5 m between each profile. The P1 profile is performed with a roll-along. P8 is placed in line with P1–P7, but further out to control whether or not the cave extends to that point. P10–P15 were placed perpendicular to the valley to determine the fill thickness.

During the three measurement campaigns, three arrays were used. In 2020 (profiles P9, P10, P11 and P12), a dipole–dipole array is used and characterized by an identical spacing (noted a) between the current and potential electrodes. The spacing between the centers of the two dipoles is a multiple of the size of the dipoles (n*a). In 2019 and 2022, two arrays were used for the other profiles. The pole-dipole array is characterized by one of the electrodes, which is placed at a great distance from the other three (referred to as the 'remote electrode'). Apart from this, the configuration is the same as for the dipole–dipole array. This array is known for its good horizontal coverage and allows fast data acquisition. The asymmetrical effect of this array is countered by operating in a direct (forward) and inverse (reverse) manner. The gradient array is more sensitive to the vertical variation of resistivity and shows a very high spatial resolution. Pole-dipole and gradient measurements aim to combine pole-dipole depth and near-surface resolution of the gradient. The dipole–dipole measurements aim to make transverse measurements in the valley and make it possible to be finer on the surface. The dipole–dipole measurements have a high sensitivity to noise at depth; it is for this reason that within the framework of the complete study of the valley, another measurement array was used.

TABLE 1 Characteristics of each ERT profiles.

Profiles	Number of electrodes	Spacing between electrodes	Profile length	Profile depth	Electrode configuration
P1-RL	120	1 m	119 m	15 m	Forward and reverse pole-dipole Gradient with roll-along (RL)
P1	72	1 m	71 m	15 m	Forward and reverse pole-dipole Gradient
P2 à P8	72	1 m	71 m	15 m	Forward and reverse pole-dipole Gradient
P9	64	0.5 m	31.5 m	6 m	Dipole–dipole
P10-P11	112	1 m	111 m	12 m	Dipole–dipole
P12	96	1 m	95 m	12 m	Dipole–dipole
P13-P14	96	0.5 m	47.5 m	13 m	Forward and reverse pole-dipole Gradient
P15	96	1 m	95 m	27 m	Forward and reverse pole-dipole Gradient

3.3 | 3D geostatistical modelling

Three-dimensional ERT using sets of orthogonal of 2D survey lines provides an efficient and cost-effective tool for site characterization in environmental and engineering investigations (Gharibi & Bentley, 2005). There are many methods to create a 3D electrical resistivity model. In the literature, the first method is called 3D ERT and has been used by Chambers et al. (2011, 2012) and Chávez et al. (2018). This method is implemented by applying a rectangular grid of electrodes with measurements in x-direction and y-direction and at an angle to the grid lines (Kneisel et al., 2014). It requires long measuring times and a very specific electrode geometrical arrangement in the field. Another method consists of building a 3D electrical image via the construction of a 2D network of a parallel and perpendicular survey lines (Kneisel et al., 2014). This method is called quasi-3D ERT. The method used in this paper is 3D geostatistical modelling, which has already been used by Verdet et al. (2020) and Xu et al. (2016). This method is based on three calculation steps. The first step consists of carrying out a preliminary study on the raw data to filter out the aberrant points. The second consists of a variographic study highlighting the spatial structuring of the data and producing a theoretical variogram. The third and final step is kriging modelling. This method is explained in detail in Verdet et al. (2020) and Xu et al. (2016). 3D geostatistical modelling allows a 3D representation of a site thanks to ERT resistivity data acquired at the La Peyrouse site. This method is used to consider anisotropy of the subsoil. Seven profiles (P1–P7) were used to carry out the geostatistical modelling with the following parameters for each of the three phases:

- study of variomaps gives an anisotropy in the vertical direction, while the horizontal plane is isotropic;
- the theoretical variogram is made up of a combination of four elementary structures: (1) a nugget effect with a sill measuring 0.0015; a spherical model with a sill of 0.0045, a horizontal range of 5 m and a vertical range of 500 m; a second spherical model with a sill of 0.03, a horizontal range of 150 m and a vertical range of 11 m; and a third spherical model simulating a nugget effect in the vertical plane with a sill of 0.0015, horizontal range 500 m and vertical range of 0.01 m; and
- kriging modelling uses a spherical neighbourhood with a 10 m diameter and an interpolation grid of 0.5*0.5*0.5.

3.4 | Other data

On this site, other studies have been carried out such as hydrogeological studies and magnetic prospecting. The hydrogeological study was carried out during the year 2022 making manual piezometric readings and also using probes installed in the various wells. These data made it possible to know where the water table is and to overcome the influence of the water table on the ERT measurements. The magnetic prospecting carried out in 2019 made it possible to highlight probably a path, that is to say that two lines marked on measurements would be the edges of a road (Hiriart et al., 2023).

4 | RESULTS

4.1 | Features of geological prospection

In total, 32 points were surveyed via geological prospection. There are 12 surveys with mechanical shovel, 7 excavations with mechanical shovel and 13 core sampling. The objective of these geological surveys is to determine the depth and the geological nature of the filling in the valley. In addition to these 32 points, it is necessary to add two new zones prospected in May 2022 by means of excavations with mechanical shovels to the right of ERT profiles P13 and P14.

Core sampling named 'C' was carried out in December 2019. They all reached the limestone bedrock except for the C7 core drilled up to 4 m deep. The limestone bedrock was likely to have been close to the bottom of the core, as a nearby geotechnical survey (S3) reached bedrock at 4.1 m depth. The geological data and sections

of core sampling are given respectively in Figure 3. Core sampling can be separated into three groups. The first group has a limestone bedrock, which is reached between 0.1 and 1 m below the natural ground. This group includes cores C1 to C5, C8 and C10. The second group reached the bedrock between 1 and 2.5 m deep, including cores C6, C12 and C20. The last group reached the bedrock between 2.5 and 4.5 m deep, including cores C7, C30 and C40, which are located in the centre of the valley. It is also important to note that the core samples C1 to C4 mainly show topsoil and no clayey materials that can be assimilated in colluvium.

The survey with mechanical shovel named 'S' was taken in 2017 by ADHA (Departmental Association of Agricultural Hydraulics). All the surveys with mechanical shovel reached the limestone bedrock (Table 2). As in the case of the core sampling, the depth of the limestone bedrock reached by the surveys with mechanical shovel can be classified into three groups. The first group (S8) reached the limestone before 1 m deep. The second group (S4 and S6) reached the limestone around 2 m deep, and the third group (the other surveys) is more than 3 m deep (maximum of 4.5 m for S3). In all the surveys with mechanical shovel, there is the presence of clays with some calcareous pebbles, which can be considered colluvium.

Excavations with the mechanical shovel named 'E' were taken in 2020 by ADHA. Excavations 1, 3, 4 and 7 reached the limestone bedrock unlike the previous attempts. The topsoil thickness, filling thickness and the depth of the limestone substrate were given in Table 2 for the geotechnical survey and excavations with mechanical shovel. The depth of the limestone bedrock reached by excavations with mechanical shovel can be classified into two groups. The first group (E3, E4 and E7) reached the limestone between 1 and 2.5 m deep. The second group (E1) between 2.5 and 3.5 m. The other excavations did not reach the limestone, as the bedrock is probably deeper. In these excavations, colluvium-type materials were found.

4.2 | ERT profiles

In total, 15 profiles were acquired in the valley. On each profile, two or three horizons have been highlighted. Two figures (Figure 4 and Figure 5) present the inversions of the ERT profiles: profiles P1 at P12 in Figure 4 and P13 at P15 in Figure 5. In this part, all profiles will be analysed and interpreted. In each profile, there is the position of core sampling, the survey with mechanical shovel and excavations with mechanical shovel, which will be used for the comparison detailed in Section 5.

The results for profiles P1 to P8 (Figure 4) are detailed because they make it possible to characterize the environment in terms of

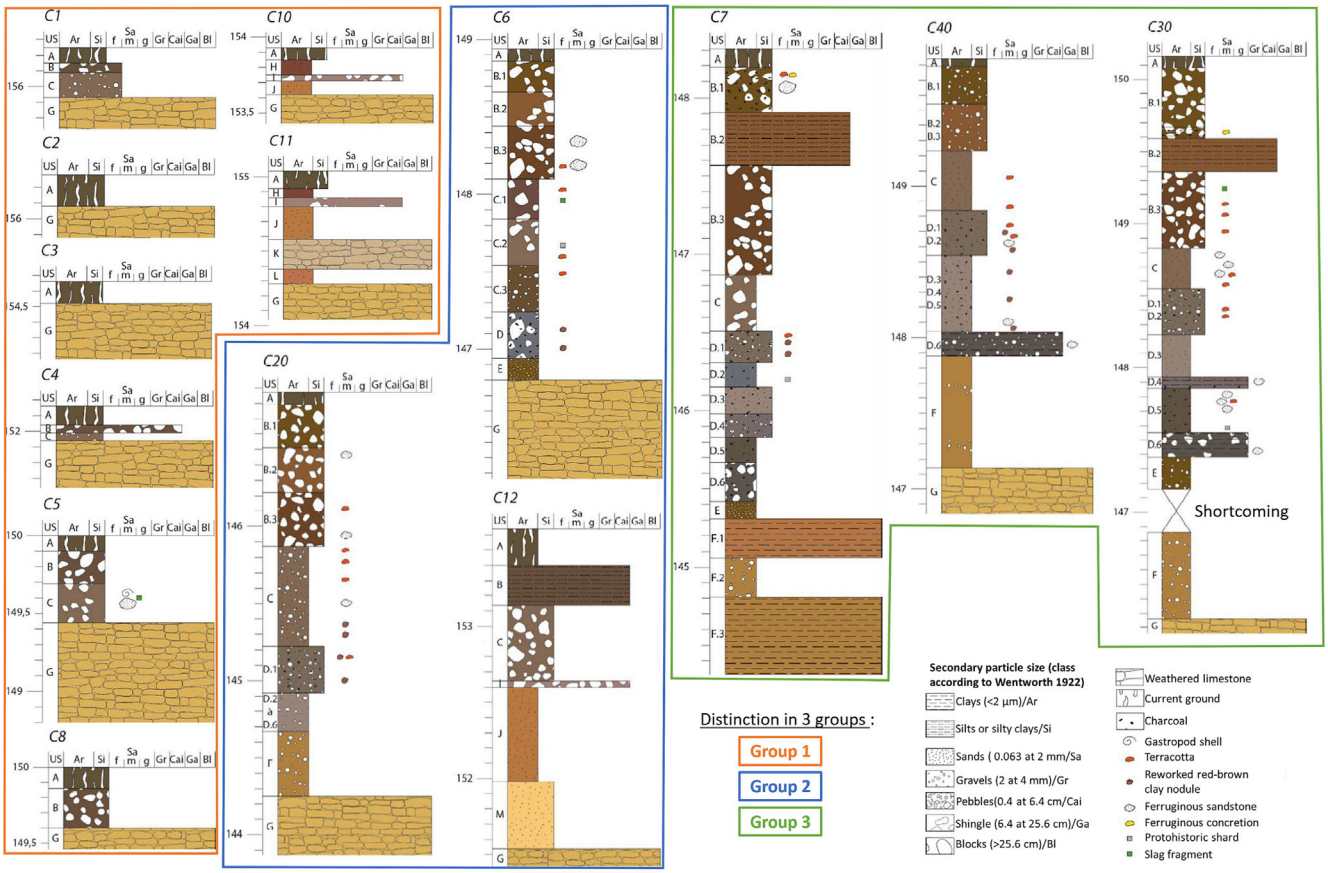

FIGURE 3 Geological cross-section and core sampling data (from Steimann) adapted by Larcanché.

TABLE 2 Summary table of characteristics of geological prospection.

Distinction in three groups	Geological surveys	Topsoil thickness	Filling thickness	Depth of limestone bedrock
Group 1	S8	0.10 m	0.9 m	1.0 m
Group 2	S4	0.10 m	1.9 m	2.0 m
	S6	0.20 m	1.8 m	2.0 m
	E3	0.20 m	1.3 m	1.5 m
	E4	0.25 m	0.8 m at 2.0 m	1 m at 2.7 m
	E7	0.25 m	1.3 m	1.5 m
Group 3	S1	0.25 m	4.0 m	4.3 m
	S2	0.15 m	3.0 m	3.2 m
	S3	0.15 m	4.3 m	4.5 m
	S5	0.10 m	3.0 m	3.1 m
	S7	0.20 m	4.0 m	4.2 m
	S9	0.10 m	1.5 m	3.6 m
	S10	0.10 m	2.6 m	3.7 m
	S11	0.10 m	4.1 m	4.2 m
	S12	0.10 m	3.5 m	3.6 m
	E1	0.25 m	2.7 m	3.2 m
	E2	0.40 m	2.4 m	Not reached
	E5	0.50 m	3.2 m	Not reached
	E6	0.40 m	3.7 m	Not reached

resistivity values. These profiles will be used for 3D geostatistical modelling. This profile consists of three horizons. Horizon 1 develops on the surface from 0 to 81 m in profile and has a resistivity of around 200 Ω·m. Horizon 2 develops under horizon 1 and 3 with a resistivity around 100 Ω·m. Horizon 3 develops on the surface in the valley, like horizon 1, between 81 and 119 m along the profile with a resistivity of less than 50 Ω·m. The limit between horizons 1 and 2 is located towards 150 m above sea level.

Profiles P2 at P8 present two horizons. Horizon 1 is characterized by a resistivity around 200 Ω·m and horizon 2 at around 100 Ω·m. The limit between these two horizons lies between 148 m above sea level (P7) and 152 m above sea level (P2). On profile P2, the surface layer shows heterogeneity around 18 m along the profile. By studying the geological map (Figure 1), it is shown that this resistive zone matches with the location of the cave. On profiles P3 to P7, a low resistivity zone in the upper layer is observable, located at 25 m (P3), 31 m (P4), 36.5 m (P5), 37.5 m (P6) and 43 m (P7); it is probably the cave, still filled with clayey sand material. On profile P8, which was made further than the other profiles P1 to P7, no trace of the cave is observable. Therefore, the hypotheses about the cave are as follows: either it is deeper than the depth reached by the profile or it does not pass through it, or it is too small to be detected or that it ends before reaching the profile. Profile P9 was produced above the cave (Figure 2) with a lower depth of investigation. This profile presents two horizons. Horizon 0 is 1 m thick with a median resistivity of about 145 Ω·m, which is a layer of topsoil, only visible via this small electrode spacing. In this horizon, there is a conductive zone (black circle on the Figure 4), which may correspond to the filled cave. Horizon 1 below horizon 0 has a median resistivity of around 200 Ω·m. The limit between these two horizons is approximately 156.5 m above sea level. It is important at this stage to highlight that with different apparatus and measuring arrays, the results found by ERT are similar.

The ERT profiles P3 to P7 (Figure 4) present conductive zones in horizon 1. These conductive zones match with the non-hollowed cave. On all the profiles P1 to P8, horizon 2 presents a more homogeneous resistivity. It could be another geological layer richer in clay, as the altitude of the boundary between these two horizons seems to agree with the boundary between the two geological layers C6e and C6d. On the P1 profile (Figure 4), seven cores and one survey with mechanical shovel are intersected. The cores C1 to C5 reach the limestone between 10 and 50 cm deep, meaning horizon 1 is characterized by limestone. The C7 coring, as mentioned in the paragraph, 'reaches' the limestone at around 4 m deep. The C6 coring and the S2 geotechnical survey reach the limestone around 3 m deep. Thanks to core drilling C6, C7 and geotechnical drilling S2, it is evident that horizon 2 is made up of limestone and horizon 3 of clays with the presence of calcareous pebbles. It is to be noted that the topsoil on the whole area is very thin.

The results for profiles P10 to P12 (Figure 4) are also detailed to characterize the environment in terms of resistivity values and establish hypotheses on the thickness of colluvium filling in the valley. These profiles exhibit three horizons. Horizon 1 is located at the surface with a resistivity of around 200 Ω·m. Horizon 3 is found in the centre of each profile, ranging from 2 to 6 m in thickness, with a resistivity of approximately 40 Ω·m. Horizon 2 lies beneath horizons 1 and 3, displaying a resistivity of around 100 Ω·m. The geological

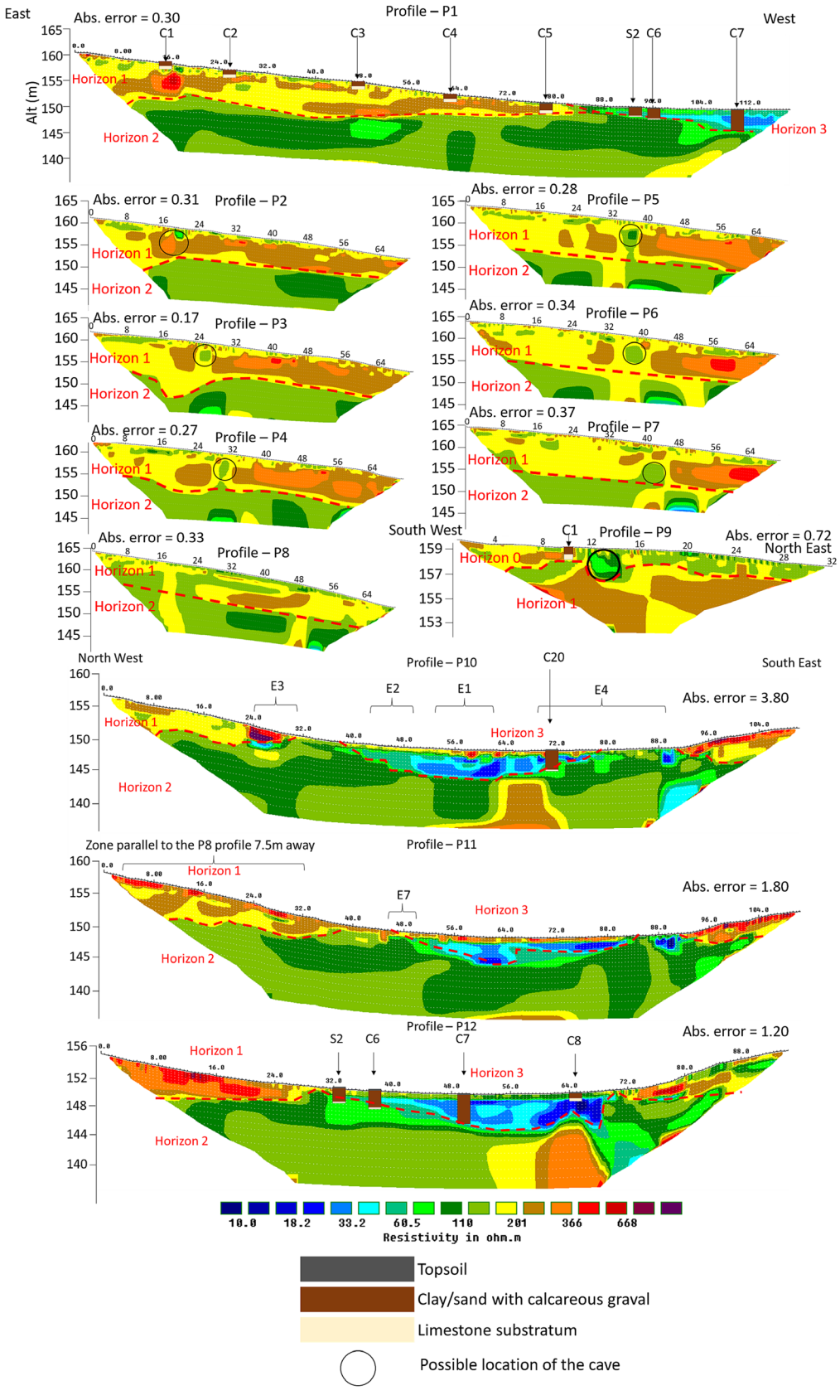

FIGURE 4 ERT profiles P1 at P12 located in Figure 2. Altitudes are given in m above sea level.

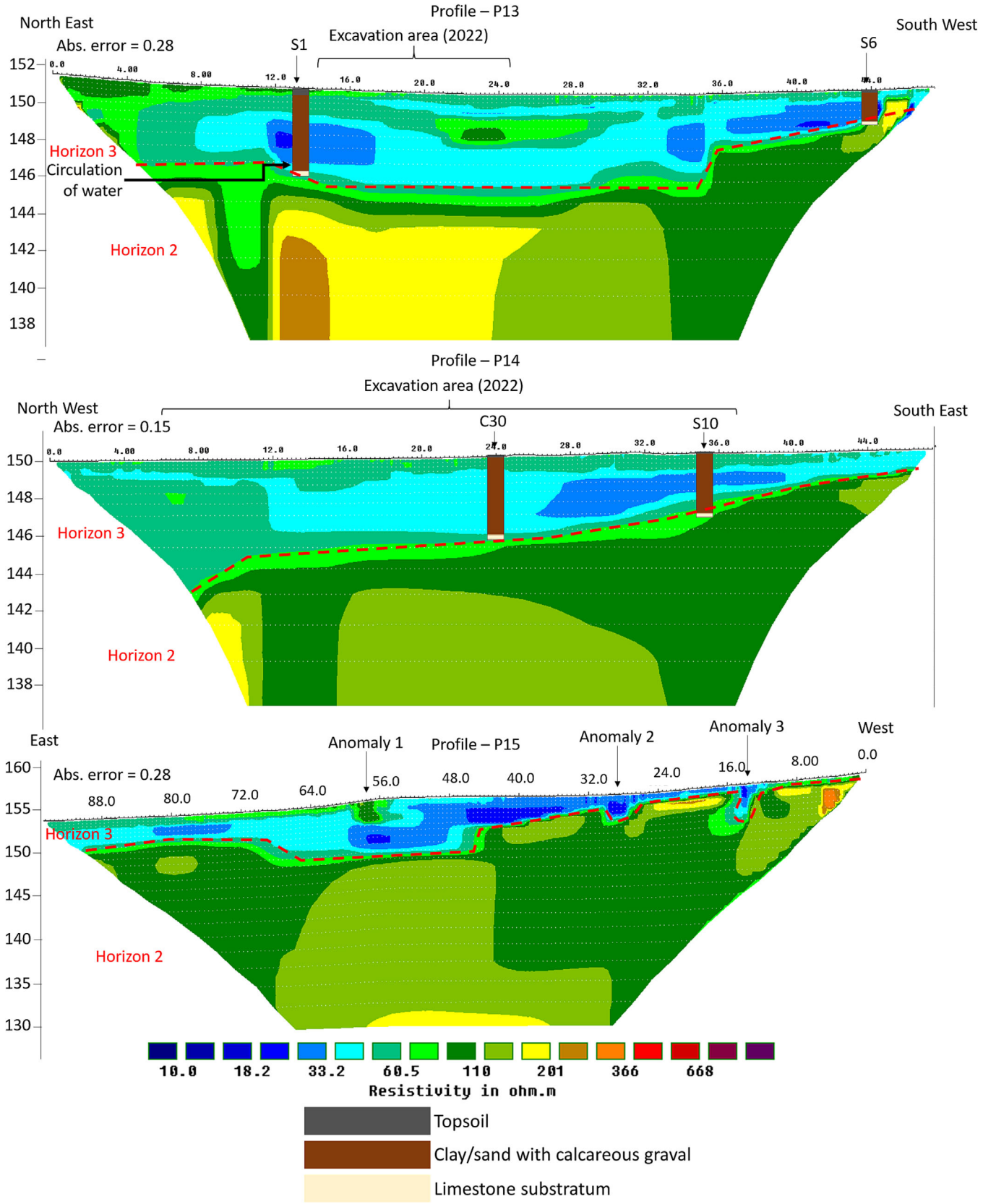

FIGURE 5 ERT profiles P14 at P15. Altitudes are given in m above sea level. The horizons are named to consistency to their equivalent in Figure 4.

interpretation of these profiles provides reliable information through geotechnical prospecting.

On profile P9, the presence of limestone is identified at a depth of 30 cm below the natural ground, indicating that horizon 1 is characterized by limestone. On profiles P10 and P12, mechanical shovel excavations and coring reveal the presence of clay with limestone gravel, followed by the limestone bedrock. Consequently, horizon 3 is associated with clays, while horizon 2 corresponds to limestone. Notably, localized pockets of limestone blocks, either without or with minimal interstitial sediment, were identified as drains on E1, E3, E4 and E6, exhibiting very high resistivities on the ERT profiles.

The results for profiles P13 to P15 (Figure 5) are presented to determine the thickness of colluvium, similar to profiles P9 to P12. These profiles also exhibit two horizons. Horizon 3 is conductive, with a resistivity of around 40 Ω·m, while horizon 2, located below horizon 3, displays a resistivity of approximately 100 Ω·m. On profile P13, horizon 3 is about 6 m thick at the centre of the valley, gradually decreasing in thickness from 36 m along the profile towards the end. On profile P14, the boundary between horizons 2 and 3 is located at a depth of 7 m to the northwest (around 8 m along the profile) and reaches a depth of 1 m to the southeast. Profile P15 shows the appearance of horizon 3 from 10 m along the profile with varying

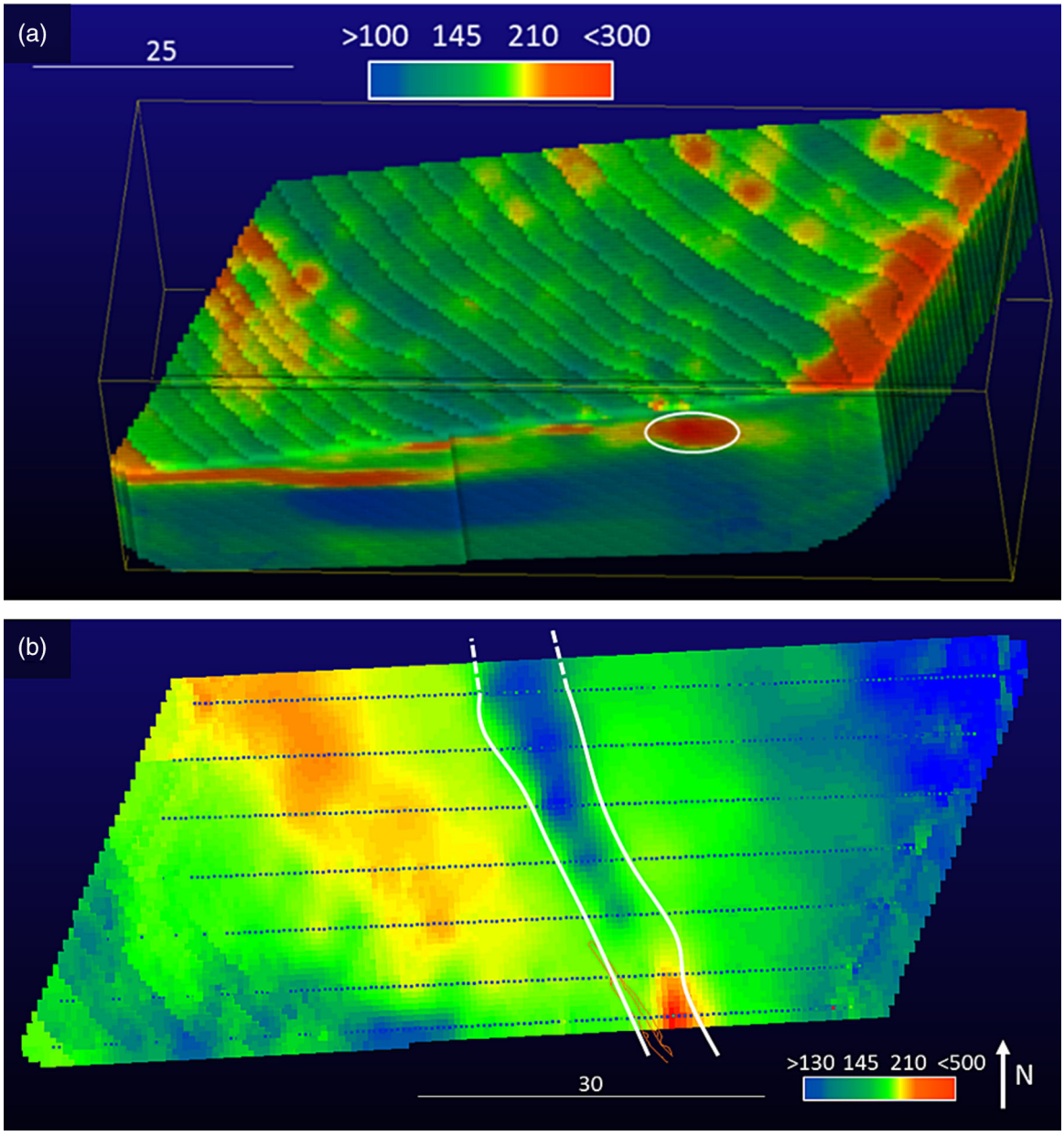

FIGURE 6 Model pictures. The values are resistivities expressed in Ω·m. (a) Complete model with the cave entrance highlighted by a white circle and (b) plan view of the model cut at 155 m above sea level. The white outlines delimit the supposed position of the cave according to the 3D modelling.

thicknesses. At 20 m along the profile, horizon 3 is 1 m thick, while at 56 m it reaches 6.5 m, and at 88 m it measures 3.5 m. A less than 1-m thick, more resistive zone is highlighted from 24 m along the profile to the western end, beneath horizon 3. By comparing these observations with core sample locations (Figure 2), it can be concluded that the centre of the valley contains a significant amount of colluvium (over 3 m), which decreases towards the valley edges (less than 50 cm).

It is important to note two geological elements discovered through these surveys regarding ERT. Firstly, water circulation in the valley is highlighted. While water was only discovered in borehole S1, between 4.1 and 4.3 m deep, just above the limestone bedrock, no water inflow was indicated during other coring operations. Profile P15 also presents three anomalies at 15, 27 and 57 m (Figure 5). Anomaly 1 corresponds to a resistive zone compared with horizon 3, potentially indicating the presence of an ancient wall according to oral sources. Two hypotheses can be proposed for anomalies 2 and 3: (1) the presence of a pipe causing water circulation in the area, as there is a well a few meters below this profile with water inlet from the north or (2) a fracture detected during previous geophysical measurements on the limestone plateau in 2019 (Hiriart & Chevillot, 2019), with a direction that may align with anomalies 2 and 3.

Therefore, according to the geological map (Figure 1), geological prospection (Table 2 and Figure 3) and ERT profiles (Figure 4 and Figure 5), horizons 1 and 2 may correspond to two different limestones, namely, C6e and C6d. With these profiles, it is possible to establish initial hypotheses. Horizon 1, with a median resistivity of around 200 Ω·m, may correspond to C6e limestone. Horizon 2, with a resistivity of around 100 Ω·m, may correspond to C6d limestone. Horizon 3, with a resistivity of about 50 Ω·m, may correspond to colluvium.

4.3 | Three-dimensional resistivity model

This geostatistical model (Figure 6) was obtained using profiles P1 to P7. Profile P1 is selected without roll-along. In this paper, only the results of this study are presented. Figure 6a presents the model in its entirety with the topography of the site, with the entrance of the cave highlighted by a white circle.

Figure 6b shows a top view of the model cut at 155 m above sea level without thresholding. This figure makes it possible to highlight the variations of resistivity for a delimited zone. To the west of the high resistivity anomaly mentioned above, there appears an anomaly of lower resistivity. From 8 m in the cave (i.e., between profiles P1 and P3; Figure 4), the cave is filled with clayey material. Thus, the continuity of the cave in terms of resistivity would be visible with a low resistivity. As a result, the cave could be visible through this low resistivity anomaly. The cave could extend to profile P7 and seems to extend beyond. The length of the cave could be 32 m with an average diameter of between 2 to 4 m. In view of this potential footprint, the cave could play a significant archaeological role within the site.

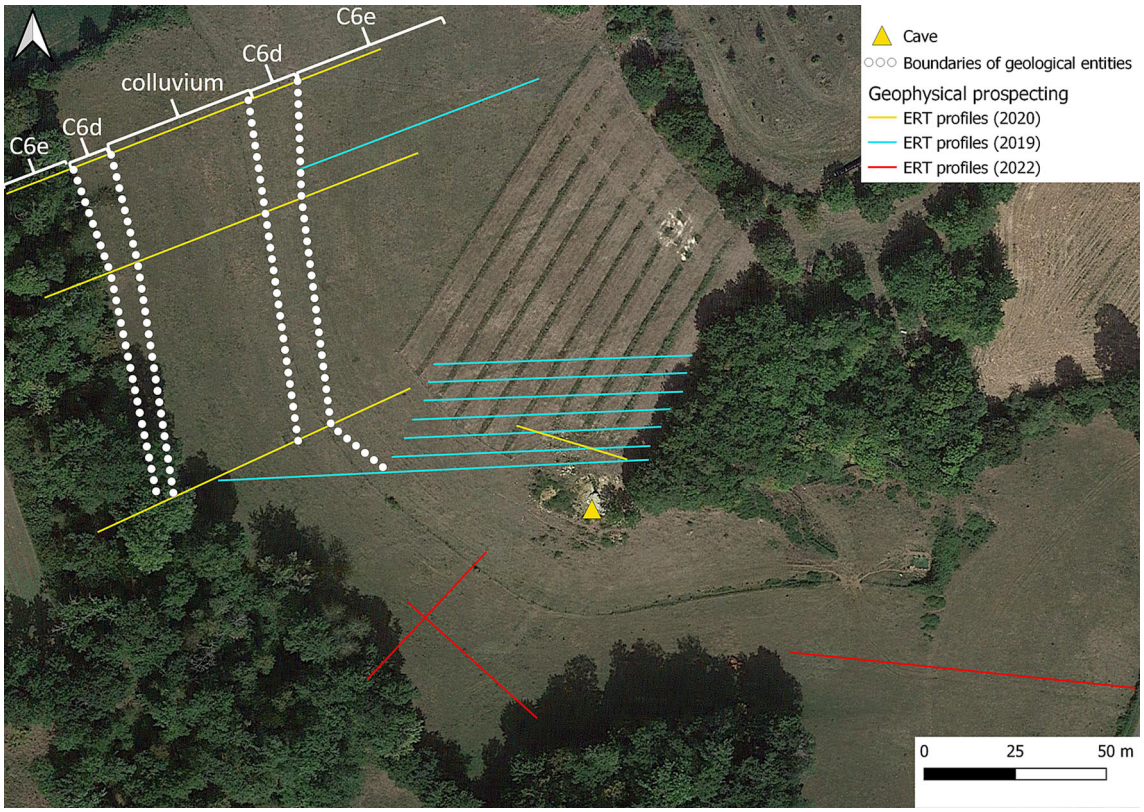

FIGURE 7 Distinction of the different geological entities present on the surface. Note that the limits were larger than the red profiles; hence, the dotted lines stop before reaching them.

5 | DISCUSSION

5.1 | Interpretations of data from a geological perspective

This study made it possible to highlight that coupling the methods firstly contributed to a better understanding of the geology and geomorphology of the site and to establish certain hypotheses. The first hypothesis mentioned in the previous part is the geological nature of the different horizons present on the ERT profiles. With these interpretations, the geological layers corresponding to C6d, C6e limestone and colluvium are highlighted. The C6d limestone is characterized by a median resistivity of 100 Ω·m, the C6e limestone by a median resistivity of 200 Ω·m and the colluvium by a median resistivity of 40 Ω·m. One of the main questions that can be raised is the presence of groundwater, which could modify the resistivity values. Therefore, the horizon with a median resistivity of 100 Ω·m may correspond to C6e limestone but containing groundwater. To answer this question, a hydrogeological study was conducted in 2021–2022. The hydrogeological study revealed 10 water points on the La Peyrouse site. These water points are wells, ponds, an aqueduct and a spring. Their water levels have made it possible to show that on this site, there are probably several aquifers (possibly a karstic zone). During the various geological soundings, the presence of water was highlighted only once (survey with mechanical shovel S1 in Figure 5). On the ERT measurements, there is no delimitation to highlight an aquifer. Thus, the horizon with a median resistivity of 100 Ω·m is not due to the presence of groundwater. This horizon is therefore not characteristic of the aquifer. This would confirm horizon 2 as the limestone from Campanian C6d.

With all the observations and interpretations made on the ERT profiles, it is possible to make a distinction between the different geological entities present on the surface with the geological map (Figure 1). These geological distinctions are only found on the ERT profiles P1 (with roll-along), P10, P11 and P12. These limits represented in a very simplified way are given on the Figure 7 by a dotted white line. It is important to highlight that on the profiles made in 2022, the edges of the C6e limestone are not reached on the ERT profiles (with the exception of the P15 profile where a thin zone under horizon 3 has a higher resistivity on the rest of the profile). Thus, with these observations, it is only possible to trace the boundaries of the geological layers on profiles P1, P10, P11 and P12 (Figure 7).

FIGURE 8 Fracturing survey and conductive zone of profile P15. Magnetic prospecting comes from (Hantrais et al., 2021).

To conclude, three horizons are visible with three distinct resistivities. The first with a resistivity of 200 Ω·m, the second of 100 Ω·m and the third of 40 Ω·m. By combining these three horizons with the geological map, the delimitation of the geological entities determined previously in Figure 7 and the geological soundings, it is possible to offer interpretations as to the geological nature of the different horizons. Thus, in view of the different ERT profiles, the horizon of median resistivity of 40 Ω m can be associated with a clay filling noted as colluvium on the geological map (Figure 1), located essentially from 145 m above sea level to the surface. In the centre of the valley, horizon of 100 Ω·m with C6d limestone is mainly below 150 m above sea level and the 200 Ω·m horizon with C6e limestone is above 150 m above sea level.

The second hypothesis is that the areas of low resistivity named 'anomaly 2 and 3' present on the ERT profile P15 may correspond to the line anomalies highlighted by magnetic prospecting at the top of the plateau (Figure 8). Indeed, excavations have revealed that these are natural fractures in the limestone. Figure 8 shows the results of magnetic prospecting with the prolongation of the fractures line and the profile P15, with anomalies 2 and 3 represented. It highlights that anomaly 2 may be characteristic of the fracture while anomaly 3 does not in fact correspond at all to it. On the other hand, as they are in close proximity with the same spacing as per the magnetic survey, excavations showed that these two anomalies correspond to fractures. Note that magnetic prospection revealed the foundation of a Celtic Sanctuary (Hiriart et al., 2023).

5.2 | Interpretations of data from an archaeological point of view

In this study, one of the main problems was to identify the thickness of the colluvium filling. As a result, it appears that the filling is located above the C6d limestone. This study also aimed to assess the evolution of the environment and human occupation of La Peyrouse over time from an archaeological perspective. During the various measurement campaigns carried out since 2014, the colluvium filling thickness has returned inconsistently. This study showed that there could potentially be around 6 m of colluvium in the centre of the valley that may have been deposited over the last few thousand years, which is hardly explained from a geomorphological point of view.

Excavations in May 2022 (delimited only with the ERT profile represented) were carried out by E. Hiriart (as part of the PCR La Peyrouse project) in the La Ruchelle valley allowing a more precise characterization of this filling (Figure 9). These excavations are positioned (named 'excavation area') on the ERT profiles P13 and P14 (Figure 5). Using this excavation, a new interpretation of the timing and the sedimentary deposits was carried out as in Mahan et al. (2023).

These large-scale excavations have made it possible to demonstrate that the 6 m of sedimentary deposits filling revealed by the ERT measurements are in fact not only colluvium but also a multilayering of archaeological levels in place, mainly from the Iron Age and the

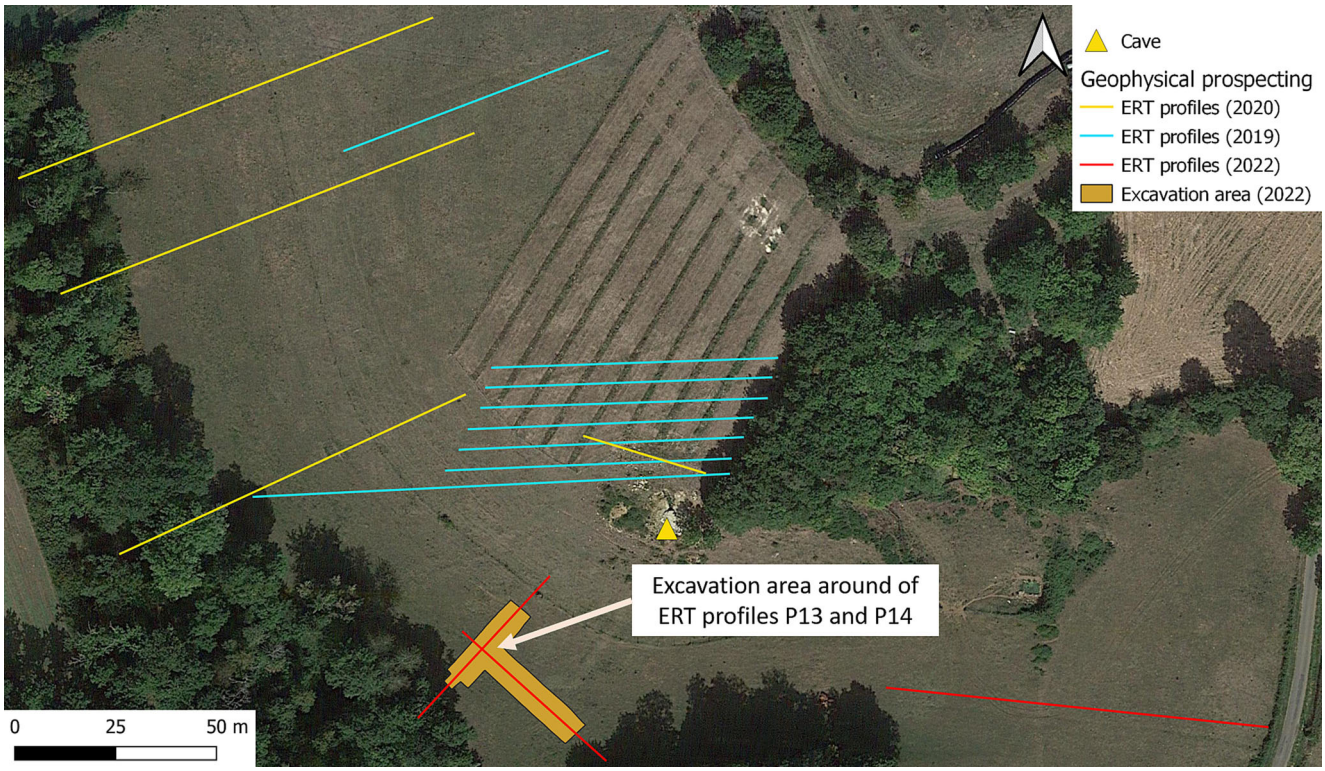

FIGURE 9 Delimitation of the excavation area in May 2022 with the representation of ERT profile in the La Ruchelle valley.

Roman period (Figure 10). Under this multiple layering of archaeological levels, clay as a result of decalcification is found. It is a geological soil but whose conductivity differs from limestone. The sector shows that in several places, the limestone is being decarbonated.

Thus, these archaeological excavations indicate that the colluvial filling is only 1.3 to 1.6 m thick over a period of approximately 2000 years. The rest of horizon 3, interpreted as colluvial filling, that is, profiles P10 to P15 with a median resistivity of 40 Ω m as discussed in the previous part (Figures 4 and 5), corresponds to the following archaeological stratigraphy: In the excavation, the level below the colluvium dates from the second century AD (Early Roman Empire). The level below dates from the Iron Age (approximately 3rd century BC) and the levels below are even older, highlighted by the discovery of a soil level dating from the Neolithic period. The different levels were not detected by geophysical methods because they are horizontal, thin (less than 50 cm) and have roughly the same geomorphological characteristics as the colluviums, that is, clayey material with the presence of limestone gravel (Figure 10). From the point of view of ERT, the presence of clay at all levels shows that in this type of situation, ERT cannot differentiate colluvium from the archaeological levels in place.

In view of the ERT profiles made in 2022 (P13 to P15) and those carried out in 2020 (P10 to P12) in the valley, horizon 3 still reaches a thickness of more than 3 m. All the observations made in this part

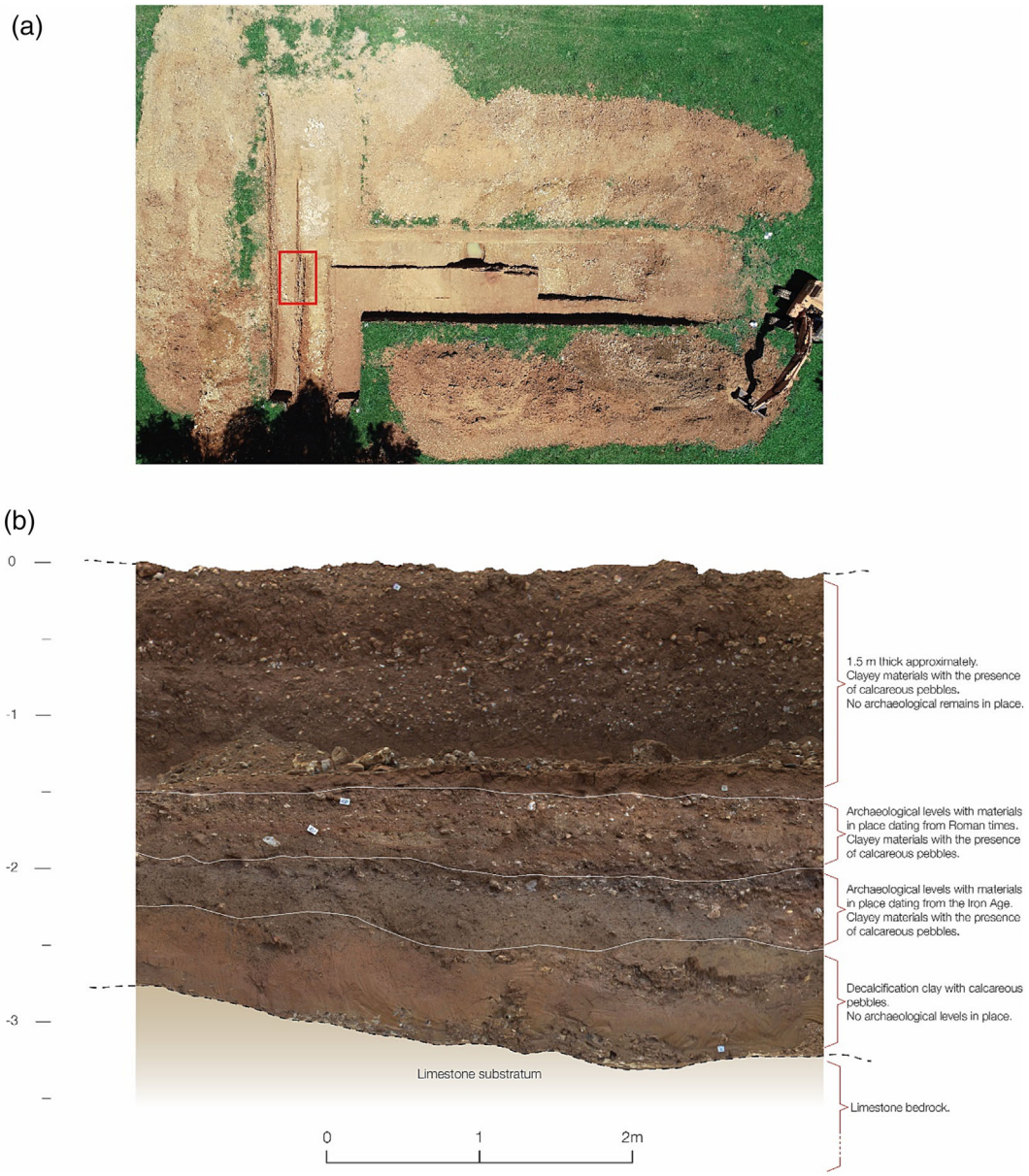

FIGURE 10 (a) Drone photograph of the excavation made in May 2022 in the valley (excavations E. Hiriart; photo C. Coutelier). (b) Section of the excavation represented by a red rectangle in (a) and showing the different archaeological levels.

have shown that the La Ruchelle valley has a lower colluvium thickness than expected, while underneath the colluvial filling, there are hypothetically archaeological remains throughout the valley dating from one to several periods depending on the occupation of this site. It is therefore possible to say that all thicknesses greater than 1.5 m with a resistivity less than 40 Ω·m could correspond to archaeological remains in place containing clay materials with limestone pebbles. Similarly, the cave at 8 m (result of 3D geostatistical modelling) has a resistivity of less than 40 Ω·m, meaning it may also correspond to a mix of archaeological remains and natural filling.

6 | CONCLUSIONS

The study of the La Peyrouse site began in 2014 with the discovery of numerous archaeological remains. In order to study the spatial extent of this exceptional site by its size (several dozen hectares), many methods have been implemented: ERT, magnetic, excavations, coring, hydrogeological survey and so on from 2019 to 2022.

The comparison of all of these data made it possible to establish an overall understanding of the site, in particular the part of the site containing the valley. Thus, by ERT measurements, the succession of two Campanian limestones (C6d and C6e) was defined. The ERT profiles carried out in the valley showed an abnormally high thickness of colluvium. From a geomorphological point of view, nothing justifies a 6 m of deposit in 2000 years. A large excavation made it possible to understand this abnormal thickness. It turns out that the colluvium is only 1.5 m thick, which is consistent with the site studied. The next 4.5 m are actually large-scale archaeological remains in a clayey-sand matrix, with a clay-limestone level below in contact with the limestone. Any abnormal information obtained via geophysics with regard to geomorphology on archaeological sites should be followed up with trenches. This set of less than 1.5 m has a resistivity of about 40 Ω·m. The ERT 3D measurements on this site have made it possible to identify a partially excavated cavity located according to the geological map between two Campanian limestones (C6d and C6e), which extends by filling with clay over a distance of 32 m. It is possible that these clays contain archaeological remains, as in the valley.

The ERT calibrated on boreholes and excavations is an excellent method for characterizing the geomorphology of a site and highlighting the geomorphological anomalies, which in this case are archaeological remains. Thanks to geophysical methods, the excavations could be well positioned. Archaeological studies at sites of such magnitude can thus be greatly assisted by establishing a morphological understanding obtained through geophysical methods.

ACKNOWLEDGEMENTS

We would like to thank Philippe Gay (site owner), Clément Coutelier and Hubert Pradier (who provided drone coverage and topography), Didier Cornaggia, Gérard Dussaud and Laurent Thieullent (amateur archaeologists whose help is invaluable), as well as Patrice Buraud and Thibaud Poigt (professional archaeologists who participated in the 2022 excavations). The research for this article would not have been possible without the financial support of New Aquitaine region (RAPSODIE project), DRAC (Ministry of Culture) General Council of the Dordogne, University of Bordeaux Montaigne and GPR Human Past.

CONFLICT OF INTEREST STATEMENT

This study has no conflicts of interest.

DATA AVAILABILITY STATEMENT

The data that support the findings of this study are available from the corresponding author upon reasonable request.

ORCID

Marie Larcanché https://orcid.org/0000-0002-3385-6505

REFERENCES

Abu-Zeid, N. (2002). Resistivity imaging in archaeology and restoration. Conf. Pap. First Int. Conf. Sci. Technol. Archeol. Conserv. Volume 1.

Apostolopoulos, G., & Kapetanios, A. (2021). Geophysical investigation, in a regional and local mode, at Thorikos Valley, Attica, Greece, trying to answer archaeological questions. *Archaeological Prospection*, *28*, 435–452. https://doi.org/10.1002/arp.1814

Becker, H. (1995). From nanotesla to picotesla — A new window for magnetic prospecting in archaeology: The Picotesla for magnetic prospecting. *Archaeological Prospection*, *2*, 217–228. https://doi.org/10.1002/1099-0763(199512)2:4<217::AID-ARP6140020405>3.0.CO;2-U

Binley, A., Keery, J., Slater, L., Barrash, W., & Cardiff, M. (2016). The hydrogeologic information in cross-borehole complex conductivity data from an unconsolidated conglomeratic sedimentary aquifer. *Geophysics*, *81*, E409–E421. https://doi.org/10.1190/geo2015-0608.1

Carrière, S. D., & Chalikakis, K. (2022). Hydrogeophysical monitoring of intense rainfall infiltration in the karst critical zone: A unique electrical resistivity tomography data set. *Data in Brief*, *40*, 107762. https://doi.org/10.1016/j.dib.2021.107762

Chambers, J. E., Wilkinson, P. B., Kuras, O., Ford, J. R., Gunn, D. A., Meldrum, P. I., Pennington, C. V. L., Weller, A. L., Hobbs, P. R. N., & Ogilvy, R. D. (2011). Three-dimensional geophysical anatomy of an active landslide in Lias group mudrocks, Cleveland Basin, UK. *Geomorphology*, *125*, 472–484. https://doi.org/10.1016/j.geomorph.2010.09.017

Chambers, J. E., Wilkinson, P. B., Wardrop, D., Hameed, A., Hill, I., Jeffrey, C., Loke, M. H., Meldrum, P. I., Kuras, O., Cave, M., & Gunn, D. A. (2012). Bedrock detection beneath river terrace deposits using three-dimensional electrical resistivity tomography. *Geomorphology*, *177–178*, 17–25. https://doi.org/10.1016/j.geomorph.2012.03.034

Chávez, R. E., Tejero-Andrade, A., Cifuentes, G., Argote-Espino, D. L., & Hernández-Quintero, E. (2018). Karst detection beneath the pyramid of El Castillo, Chichen Itza, Mexico, by non-invasive ERT-3D methods. *Scientific Reports*, *8*, 15391. https://doi.org/10.1038/s41598-018-33888-9

Dahlin, T. (2000). Short note on electrode charge-up effects in DC resistivity data acquisition using multi-electrode arrays: Short note on electrode charge-up effects. *Geophysical Prospecting*, *48*, 181–187. https://doi.org/10.1046/j.1365-2478.2000.00172.x

Dalan, R. A., & Banerjee, S. K. (1996). Soil magnetism, an approach for examining archaeological landscapes. *Geophysical Research Letters*, *23*, 185–188. https://doi.org/10.1029/95GL03689

Deiana, R., Leucci, G., & Martorana, R. (2018). New perspectives on geophysics for archaeology: A special issue. *Surveys in Geophysics*, *39*, 1035–1038. https://doi.org/10.1007/s10712-018-9500-4

Eppelbaum, L. V., Khesin, B. E., & Itkis, S. E. (2001). Prompt magnetic investigations of archaeological remains in areas of infrastructure development: Israeli experience. *Archaeological Prospection*, *8*, 163–185. https://doi.org/10.1002/arp.167

Gharibi, M., & Bentley, L. R. (2005). Resolution of 3-D electrical resistivity images from inversions of 2-D orthogonal lines. *Journal of Environmental and Engineering Geophysics*, *10*, 339–349. https://doi.org/10.2113/JEEG10.4.339

Gunther, T., & Rucker, C. (2012). Electrical Resistivity Tomography (ERT) in geophysical applications - state of the art and future challenges. Conf. Pap.

Hantrais, J., Mathé, V., & Corfmat, P. (2021). Regards croisés sur le sanctuaire laténien de La Peyrouse (Saint-Félix-de-Villadeix, Dordogne): confrontation des données géophysiques et archéologiques. *ArchéoSciences*, *45*(2), 43–54. https://doi.org/10.4000/archeosciences.10527

Hiriart, E., & Chevillot, C. (2019). Les opérations archéologiques menées à La Peyrouse (Saint-Félix-de-Villadeix, Dordogne) en 2019. Rapport final d'opération. [Rapport de recherche] Région Nouvelle-Aquitaine; Ministère de la Culture et de la Communication, DRAC-SRA Nouvelle-Aquitaine; Université Bordeaux Montaigne; ADRAHP; Cnrs; ADRAHP; Université de La Rochelle; LIENSs (UMR 7266). pp.682. ⟨hal-02456541⟩.

Hiriart, E., Chevillot, C., Hantrais, J., Bertaud, A., Brochot, M., Corbasson, C., Demierre, M., Fabiani, M., Loirat, D., Mounier, A., Olmer, F., Rolland, J., Rousseau, É., Sarrazin-Robert--Dejeans, J.-C., Valette, R., & Mathé, V. (2022). Un premier sanctuaire celtique en Aquitaine. Résultats des fouilles menées en 2020 sur l'agglomération ouverte de La Peyrouse (Saint-Félix-de-Villadeix, Dordogne). Aquitania 38.

Hiriart, E., Hantrais, J., Beyrie, A., Chevillot, C., Colin, S., Fabre, J.-M., Glais, A., Larcanché, M., Leroyer, C., Lopez, S., Paillou, P., Sirieix, C., Steinmann, R., Verdet, C., & Mathé, V. (2023). First results from the sites of La Peyrouse and Blis (Dordogne).

Hojat, A., Loke, M.H., Karimi Nasab, S., Ranjbar, H., & Zanzi, L. (2020). Two-dimensional ERT simulations to compare different electrode configurations in detecting qanats. 3rd Asia Pacific Meeting on Near Surface Geoscience & Engineering, Chiang Mai, Thailand. https://doi.org/10.3997/2214-4609.202071056

Jongmans, D., & Garambois, S. (2007). Geophysical investigation of landslides: A review. *Bulletin de la Société Géologique de France*, *178*, 101–112. https://doi.org/10.2113/gssgfbull.178.2.101

Kneisel, C., Emmert, A., & Kästl, J. (2014). Application of 3D electrical resistivity imaging for mapping frozen ground conditions exemplified by three case studies. *Geomorphology*, *210*, 71–82. https://doi.org/10.1016/j.geomorph.2013.12.022

Kofman, L., Ronen, A., & Frydman, S. (2006). Detection of model voids by identifying reverberation phenomena in GPR records. *Journal of Applied Geophysics*, *59*, 284–299. https://doi.org/10.1016/j.jappgeo.2005.09.005

Leucci, G., de Giorgi, L., di Giacomo, G., Ditaranto, I., Miccoli, I., & Scardozzi, G. (2016). 3D GPR survey for the archaeological characterization of the ancient Messapian necropolis in Lecce, South Italy. *Journal of Archaeological Science: Reports*, *7*, 290–302. https://doi.org/10.1016/j.jasrep.2016.05.027

Loke, M. H., & Barker, R. D. (1996). Rapid least-squares inversion of apparent resistivity pseudosections by a quasi-Newton method1. *Geophysical Prospecting*, *44*, 131–152. https://doi.org/10.1111/j.1365-2478.1996.tb00142.x

Mahan, S., Wood, J. R., Lovelace, D. M., Laden, J., McGuire, J. L., & Meachen, J. A. (2023). Luminescence ages and new interpretations of the timing and deposition of Quaternary sediments at natural trap Cave, Wyoming. *Quaternary International*, *647–648*, 22–35. https://doi.org/10.1016/j.quaint.2022.01.005

Pánek, T., Margielewski, W., Tábořík, P., Urban, J., Hradecký, J., & Szura, C. (2010). Gravitationally induced caves and other discontinuities detected by 2D electrical resistivity tomography: Case studies from the Polish Flysch Carpathians. *Geomorphology*, *123*, 165–180. https://doi.org/10.1016/j.geomorph.2010.07.008

Park, M. K., Park, S., Yi, M.-J., Kim, C., Son, J.-S., Kim, J.-H., & Abraham, A. A. (2014). Application of electrical resistivity tomography (ERT) technique to detect underground cavities in a karst area of South Korea. *Environment and Earth Science*, *71*, 2797–2806. https://doi.org/10.1007/s12665-013-2658-7

Perrone, A., Iannuzzi, A., Lapenna, V., Lorenzo, P., Piscitelli, S., Rizzo, E., & Sdao, F. (2004). High-resolution electrical imaging of the Varco d'Izzo earthflow (southern Italy). *Journal of Applied Geophysics*, *56*, 17–29. https://doi.org/10.1016/j.jappgeo.2004.03.004

Querrien, A., Moulin, J., & Tabbagh, A. (2009). Confrontation of geophysical survey, soil studies and excavation data to evidence tillage erosion. *ArchéoSciences*, *33*, 195–198. https://doi.org/10.4000/archeosciences.1576

Rousset, D., Genthon, P., Perroud, H., & Sénéchal, G. (1998). Detection and characterization of near surface small karstic cavities using integrated geophysical surveys. 4th Meet. Environ. Eng. Geophys. Soc. 367–370. https://doi.org/10.3997/2214-4609.201407122

Schrott, L., Otto, J.-C., Götz, J., & Geilhausen, M. (2013). 14.2 fundamental classic and modern field techniques in geomorphology: an overview. In *Treatise on geomorphology* (pp. 6–21). Elsevier. https://doi.org/10.1016/B978-0-12-374739-6.00369-9

Trinks, I., Hinterleitner, A., Neubauer, W., Nau, E., Löcker, K., Wallner, M., Gabler, M., Filzwieser, R., Wilding, J., Schiel, H., Jansa, V., Schneidhofer, P., Trausmuth, T., Sandici, V., Ruß, D., Flöry, S., Kainz, J., Kucera, M., Vonkilch, A., … Seren, S. (2018). Large-area high-resolution ground-penetrating radar measurements for archaeological prospection. *Archaeological Prospection*, *25*, 171–195. https://doi.org/10.1002/arp.1599

Tsourlos, P. I., & Tsokas, G. N. (2011). Non-destructive electrical resistivity tomography survey at the south walls of the acropolis of Athens: Electrical resistivity tomography survey at the acropolis of Athens. *Archaeological Prospection*, *18*, 173–186. https://doi.org/10.1002/arp.416

Verdet, C., Sirieix, C., Marache, A., Riss, J., & Portais, J.-C. (2020). Detection of undercover karst features by geophysics (ERT) Lascaux cave hill. *Geomorphology*, *360*, 107177. https://doi.org/10.1016/j.geomorph.2020.107177

Wentworth, C. K. (1922). A scale of grade and class terms for clastic sediments: the canonical definition of sediment grain sizes as defined by geologist Chester K. Wentworth.

Xu, S., Sirieix, C., Ferrier, C., Lacanette-Puyo, D., Riss, J., & Malaurent, P. (2015). A geophysical tool for the conservation of a decorated cave - a case study for the Lascaux Cave: Conservation of Lascaux Cave using ERT survey. *Archaeological Prospection*, *22*, 283–292. https://doi.org/10.1002/arp.1513

Xu, S., Sirieix, C., Marache, A., Riss, J., & Malaurent, P. (2016). 3D geostatistical modeling of Lascaux hill from ERT data. *Engineering Geology*, *213*, 169–178. https://doi.org/10.1016/j.enggeo.2016.09.009

How to cite this article: Larcanché, M., Verdet, C., Sirieix, C., Steinmann, R., Colin, S., Mathé, V., Chevillot, C., Matéo, S., Houillon, N., Hantrais, J., & Hiriart, E. (2023). A Late Holocene case study from south-west France: Combining geomorphology and geophysics to understand archaeological site morphology. *Archaeological Prospection*, *30*(4), 517–532. https://doi.org/10.1002/arp.1913